



HAL
open science

Theoretical description of cluster formation in two-Yukawa competing fluids

Dino Costa, Carlo Caccamo, Jean-Marc Bomont, Jean-Louis Bretonnet

► **To cite this version:**

Dino Costa, Carlo Caccamo, Jean-Marc Bomont, Jean-Louis Bretonnet. Theoretical description of cluster formation in two-Yukawa competing fluids. *Molecular Physics*, 2011, pp.1. 10.1080/00268976.2011.611480 . hal-00739201

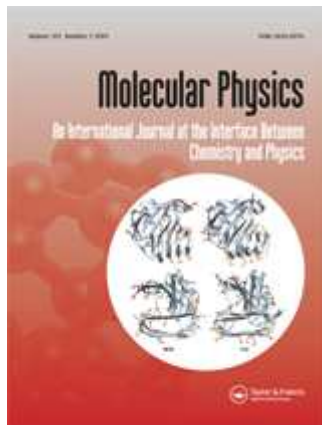
HAL Id: hal-00739201

<https://hal.science/hal-00739201>

Submitted on 6 Oct 2012

HAL is a multi-disciplinary open access archive for the deposit and dissemination of scientific research documents, whether they are published or not. The documents may come from teaching and research institutions in France or abroad, or from public or private research centers.

L'archive ouverte pluridisciplinaire **HAL**, est destinée au dépôt et à la diffusion de documents scientifiques de niveau recherche, publiés ou non, émanant des établissements d'enseignement et de recherche français ou étrangers, des laboratoires publics ou privés.



Theoretical description of cluster formation in two-Yukawa competing fluids

| | |
|--|--|
| Journal: | <i>Molecular Physics</i> |
| Manuscript ID: | TMPH-2011-0217.R1 |
| Manuscript Type: | Special Issue in honour of Luciano Reatto |
| Date Submitted by the Author: | 25-Jul-2011 |
| Complete List of Authors: | Costa, Dino; Università di Messina, Dipartimento di Fisica Caccamo, Carlo; Università di Messina, Dipartimento di Fisica Bomont, Jean-Marc; Universite Paul Verlaine, Institut de Physique Bretonnet, Jean-Louis; Université Paul Verlaine, Laboratoire de Physique des Milieux Denses |
| Keywords: | competing interactions, non-homogeneous phases, cluster formation, theory of the liquid state |
| <p>Note: The following files were submitted by the author for peer review, but cannot be converted to PDF. You must view these files (e.g. movies) online.</p> <p>source files.zip</p> | |

SCHOLARONE™
Manuscripts

REPLY TO REFEREE REPORT OF PAPER TMPH-2011-0217

We have carefully amended the original version of paper TMPH-2011-0217 according to the advice of the referee. A point-to-point report of all corrections is given below. For the clarity sake, all modifications are reported in red colour both in this reply and in the revised manuscript.

§ § §

Referee. Point 1-i: Throughout the paper, the situation in which the structure factor displays the small- q peak due to cluster-cluster correlation is referred to as pertaining to a “non-homogeneous fluid” or a “non homogeneous phase”, as opposed to the “homogeneous fluid”, in which such a peak is absent [...]. However, the occurrence of such a peak does not correspond in itself to a phase transition between a homogeneous and a non homogeneous phase, and the fluid is actually homogeneous for all the states considered here, including those for which the small- q peak of the structure factor is present [...]. I think that this point should be made clearer in the manuscript. In most cases, this will simply amount to a different choice of the words used to design the situation in which cluster formation occurs, yet I think it is well worth doing so.

Reply: We agree with the Referee that the cluster formation investigated in this work does not give rise to a thermodynamically resolved phase transition, and therefore the words “non-homogeneous phase” constitutes a misleading expression. To avoid confusion, we have designated throughout the paper the situation in which the cluster formation occurs as a “cluster fluid”. This expression is first defined in the Introduction of the revised version (page 2) as:

clusters start to develop out of the fluid phase, giving rise to what we term in the rest of the paper “cluster fluid”.

§ § §

Referee. Point 1-ii: The above observation also prompts the natural question, of how the (real) phase transition to the non homogeneous phase will come along in the present treatment. I suspect that, if the temperature is taken to values lower than those considered here, the integral equations, either MHNC or BB, will eventually fail to converge, but some

1
2
3 more information would definitely be welcome, even without going into detail. For instance,
4 if this is the case, at what temperatures would the theories fail to converge? Are they much
5 lower than the lowest temperatures investigated here? And how big will the cluster peak
6 be by the time this happens? The structure factors shown in Fig. 4 do certainly show the
7 cluster peak, but its value is relatively small, in particular smaller than that of the peak
8 related to particle-particle correlations.
9

10
11
12
13
14 **Reply:** We have added a comment, also taking into account the conclusions of previous
15 studies [29,36], clarifying the expected behaviour of the system at low enough tempera-
16 tures and the corresponding performances of the BB and MHNC approximations. The new
17 sentence (page 7) reads:
18
19
20

21
22 On the other hand, since our models have a long-range repulsive contribution
23 (non negligible up to $r \sim 4\sigma$), the system is expected to form [29], for low enough
24 temperatures, a Wigner glass of clusters, i.e. a disordered state of polydisperse
25 clusters that do not percolate to give a gel. The investigation of this regime
26 is substantially out of the scope of the theoretical framework employed in this
27 work; moreover, as shown in Ref. [36], the BB algorithms ceases to numerically
28 converge for temperatures approximately around $T^* = 0.30$ (i.e. close to the
29 lowest temperatures reported in Figure 4), and test calculations (not reported
30 here) demonstrate that the same limiting temperature range holds for the MHNC
31 approximation.
32
33
34
35
36
37
38
39
40

41 § § §
42
43
44

45 **Referee. Point 2:** One might want to observe that, while the lower temperatures at
46 which the structure factor was studied are close to or even lower than the critical tem-
47 peratures of the purely attractive fluid estimated by the Noro-Frenkel rule, the structure
48 factor at $k=0$ always remains much lower than unity, and the second virial coefficient is
49 always positive. This would help substantiate the statement made in the last paragraph of
50 the conclusions, that “the liquid-vapor coexistence . . . completely disappears in favor of the
51 microsegregation, once the full 2Y interactions is taken into account”.
52
53
54
55
56

57 **Reply:** We thank the Referee for his suggestion; we have simply deemed as more appro-
58 priate to cite his remark in the Results section, where we discuss the various features of the
59
60

1
2
3 structure factor (i.e. in connection with Figure 4), leaving untouched the Conclusions. We
4
5 have in particular added the sentence (page 7):
6
7

8 As visible from Figure 4, while the lower temperatures at which the structure
9 factor is studied are close to or even lower than the critical temperatures of the
10 purely attractive fluid estimated by the Noro-Frenkel rule, the $k \rightarrow 0$ limit of
11 the structure factor, directly related to the isothermal compressibility, always
12 remains much lower than unity. This evidence (together with the fact that the
13 second virial coefficient is always positive, see Figure 2b), further corroborates
14 our previous statement about the absence of a liquid-vapour phase separation.
15
16
17
18
19

20
21 § § §
22
23

24 **Referee, Point 3:** In the review of theoretical studies on microphase formation given
25 in the Introduction, I think that also the work by A. Ciach deserves mention, see A. Ciach,
26 Phys. Rev. E 78, 061505 (2008); A. Ciach and W. T. Gozdz, Cond. Matt. Phys. 13, 23603
27 (2010); A. Ciach, Mol. Phys. 109, 1101 (2011).
28
29
30

31 **Reply:** We agree with the Referee and therefore we have added (page 2) a new sentence
32 shortly making reference to the work of A. Ciach and collaborators (new citations 24, 25
33 and 26):
34
35
36

37 At low enough temperatures, a universal sequence of cluster phases (compris-
38 ing ordered, periodic bcc, hexagonal and lamellar phases), and the existence of
39 a gyroid phase (possibly related to a network-forming cluster of colloids in col-
40 loid/polymer mixtures) were predicted in Refs. [24,25] by means of a mesoscopic,
41 coarse-grain theory for soft materials combining density functional and statisti-
42 cal field theory; more recently, the same formalism was used to investigate the
43 general features of microscopic interaction potentials leading to inhomogeneous
44 structures [26].
45
46
47
48
49
50
51

52
53 § § §
54
55

56 **Referee, Point 4:** In Sec. 2.1, it is explained that z_2 has been chosen so as to give the
57 same behavior for B_2 . Has the choice of z_2 been made by visual inspection? Or has some
58 different criterion been used?
59
60

Reply: Indeed, in the original manuscript we omitted a description of the procedure followed to calculate z_2 . We have remedied this point with the new sentence (page 4):

In particular, we have chosen three different z_1 values (i.e. $z_1 = 19$, model M1 hereafter; $z_1 = 13$, model M2; $z_1 = 10$, model M3) and freely fixed $z_2 = 0.5$ for $z_1 = 10$, as in Ref. [36]; then, we have identified the remaining two z_2 values (to within a $\Delta z_2 = 0.001$ resolution) as those minimizing the variance between the various B_2 in the temperature range $[0.4 - 0.8]$.

For the clarity sake, we have also slightly rearranged the rest of the same paragraph.

§ § §

Referee, Point 5: Below Eq. (9), a simplified MHNC scheme is mentioned, where σ_{HS} was determined without imposing thermodynamic self-consistency. How was σ_{HS} determined, then? Was it taken equal to the true hard-sphere diameter?

Reply: We have revised the sentence after Eq. (9) to exactly account for the procedure followed by Archer and Wilding in current Ref. [20]:

An application of a simplified, thermodynamically non-consistent MHNC scheme to 2Y fluids — with $B(r)$ in Eq. (9) given by the PY expression for the hard-sphere fluid bridge function at the same density [42,43] — is also reported in Ref. [20].

§ § §

Referee, Point 6: In Sec. 3, the Noro and Frenkel rule of corresponding states is mentioned. I suggest to add a quick reminder of what this rule consists of.

Reply: A quick reminder is certainly useful: we have added the following sentence about the Noro-Frenkel rule (page 6):

The empirical rule determined by Noro and Frenkel in Ref. [56] — well verified by a wide class of central potentials — states a linear relationship between the range of a given interaction potential and the corresponding critical temperature, once (i) the critical temperature is expressed in terms of the depth of the potential well (as in our previous definition of T^*) and (ii) the range of the potential

1
2
3 is expressed in terms of an equivalent square-well interaction having the same
4 reduced second virial coefficient $B_2(T^*)/B_2^{\text{HS}}$ [see Eq. (4)] at the same reduced
5 temperature T^* .
6
7

8
9
10 § § §
11

12 **Referee, Point 7:** Pg. 7, line 11: “the cluster peak heralds ...”: perhaps “the cluster
13 peak appears ...”?

14
15 **Reply:** We used “it heralds” meaning “it becomes more and more prominent”, rather
16 than “it appears”. For the clarity sake we have used in the revised version the expression
17 (page 7, line 22) **develops significantly**.
18
19
20
21

22 § § §
23
24

25 **Referee, Point 8:** Pg. 7, line 37: “(see Figure 3)”: I assume it is Figure 3 of Ref. [32].

26
27 **Reply:** We erroneously referred to Figure 3 of the manuscript rather than to Figure 1,
28 reproducing the same models used in old Ref. [32] (current Ref. [36]). We have corrected
29 and clarified this point by using:
30
31
32

33 (see Figure 1, reproducing the models adopted in Ref. [36])
34
35

36 § § §
37
38

39 **Referee, Point 9:** Pg. 7, line 44: “...at higher packings the formation of clusters is
40 hampered by strong repulsion and thermal motion ...”: actually, the thermal motion, as
41 expressed by the average particle speed, should be independent of density.
42
43
44

45 **Reply:** We have removed from page 8 (line 21) of the revised version the words “and
46 thermal motion”.
47
48
49
50
51
52
53
54
55
56
57
58
59
60

RESEARCH ARTICLE

Theoretical description of cluster formation
in two-Yukawa competing fluidsD. Costa^{a*} C. Caccamo^a, J.-M. Bomont^b and J.-L. Bretonnet^b^a*Dipartimento di Fisica, Università degli Studi di Messina
Viale F. Stagno d'Alcontres 31, 98166 Messina, Italy*^b*Laboratoire de Physique des Milieux Denses, Université Paul Verlaine
1 Bd. Arago, 57078 Metz, France**(Received 00 Month 200x; final version received 00 Month 200x)*

We investigate the temperature threshold whereupon two-Yukawa fluids with microscopic competing interactions transform from normal to cluster fluids. Specifically, we apply two refined, thermodynamically self-consistent integral equation theories of the liquid state to study a family of two-Yukawa models having the same interaction strength, independently on the choice of potential parameters. We find, over the range of potential parameters and fluid densities investigated, an almost linear scaling between the temperature threshold for the cluster formation and the height of repulsive interactions, with higher barriers stabilizing the cluster fluid at higher temperatures. Cluster-cluster correlation lengths seem instead influenced by the long-range features of interactions.

Keywords: competing interactions; non-homogeneous phases; cluster formation; theory of the liquid state.

1. Introduction

Microscopic competing interactions are characterized by the presence, in the overall particle-particle potential, of attractive and repulsive contributions (generally beside an excluded volume term) acting on different length scales. Such peculiar interactions are ubiquitous in soft materials: as few examples, they were used to model protein solutions [1–5], colloids [1, 6, 7], star polymers [8]. The long-range repulsion is generally attributed to the weakly screened charge carried by the colloidal molecules, or to the presence of cosolutes in the solution [9], whereas the short-range attraction arises from several different mechanisms, including van der Waals interactions, depletion forces, hydrophobic effects [10–12]. Perhaps the most intriguing effect related to the presence of such competing interactions is the large variety of different fluid phases they can give rise, including (besides normally homogeneous phases) patterned or modulated phases and other locally inhomogeneous states characterized by the presence of stripes, bubbles, lamellæ or clusters (see e.g. the review [13]).

Several aspects of the rich phenomenology exhibited by fluids with competing interactions were elucidated by Luciano Reatto and coworkers in the last decade,

*Corresponding author. Email: dcosta@unime.it

1 by means of a variety of theoretical and simulation techniques. As a few exam-
2 ples, in models exhibiting a normal liquid-vapour phase separation they found a
3 great expansion of the temperature-density region around the critical point where
4 the system experiences large density fluctuations and a remarkable enhancement
5 of the short-range correlations, in comparison with a fluid with purely attractive
6 interactions [14, 15]. First and second order phase transitions from a uniform fluid
7 to a modulated inhomogeneous phase were described in [16]. Spontaneous pat-
8 tern formation, and the effect of shear on the formation and stability of clusters
9 and stripes in bidimensional systems were analysed in Refs. [17] and [18], respec-
10 tively. The interfacial properties of fluids with competing interactions, as the den-
11 sity profiles at the planar liquid-gas interface or fluids adsorbed at a planar hard
12 wall, were investigated in Ref. [19]. In order to further extend this overview, we
13 mention the possibility to observe a first-order transitions separating the vapour
14 from a fluid of spherical liquid-like clusters or the liquid from a fluid of spherical
15 voids [20]. Theoretical studies [21] predicted that model colloidal particles con-
16 fined to an interface such as the air-water interface have a bulk phase diagram
17 exhibiting clusters, stripes, and bubble modulated phases, in addition to homoge-
18 neous fluid phase and a rather complex phase behaviour upon confinement. The
19 prediction of lamellar order, microphase structures, and glassy phases in a field
20 theoretic model for charged colloids was reported in Refs. [22, 23], suggesting that
21 the cluster phase observed in such systems might be the signature of an underlying
22 equilibrium lamellar phase, hidden on the experimental time scale. **At low enough**
23 **temperatures, a universal sequence of cluster phases (comprising ordered, periodic**
24 **bcc, hexagonal and lamellar phases), and the existence of a gyroid phase (possibly**
25 **related to a network-forming cluster of colloids in colloid/polymer mixtures) were**
26 **predicted in Refs. [24, 25], by means of a mesoscopic, coarse-grain theory for soft**
27 **materials combining density functional and statistical field theory; more recently,**
28 **the same formalism was used to investigate the general features of microscopic**
29 **interaction potentials leading to inhomogeneous structures [26].** Investigations in
30 this area attracted increasing attention also because they may shed light on ag-
31 gregation phenomena that can precede arrested states [27–34]; more generally, the
32 control of aggregation processes constitutes a crucial step in disparate realms of
33 science and technology, e.g. in colloid and polymer science, in the study of human
34 diseases caused by the formation of fibrillar aggregates, in the protein structure
35 determination, in the production of photonic crystals, in food science. We refer the
36 interested reader to Refs. [20, 35, 36] for an up-to-date bibliography accounting
37 quite extensively for the last three decades studies on this topic.

38 In this work, we focus on the phenomenon of cluster formation, particularly
39 regarding the temperature threshold whereupon **clusters start to develop out of**
40 **the fluid phase, giving rise to what we term in the rest of the paper “cluster fluid”.**
41 The onset of aggregation is experimentally signalled by the appearance of a low-
42 wavevector peak in the static structure factor of the fluid (cluster peak), beside the
43 main particle-particle correlation peak [1, 27, 30]. Theoretical studies interpreted
44 the development of such low- k peak in terms of enhanced density fluctuations that,
45 at variance with the purely attractive case, do not evolve into a fully developed
46 macroscopic phase separation [6, 14, 17]; therefore, the formation of aggregates in
47 the fluid phase results from an appropriate balance between attraction, favouring
48 the cluster growth at low enough temperature, and long-range repulsion, preventing
49 a complete phase separation.

50 A widely studied prototype system exhibiting competing interactions is repre-
51 sented by the two-Yukawa (2Y) model — see Eq. (1) in the next section — where
52 the competition is obtained from the sum of two Yukawa screened interactions with
53
54
55
56
57
58
59
60

different amplitudes and decay lengths, see e.g. [5, 14–21, 28, 36–40]. Several of such studies involved an investigation of the model based on a systematic variation of one or more potential parameters, not necessarily implying a corresponding systematic variation of the overall shape of the 2Y potential itself (see e.g. Figure 1 in the next section). We here assume a different viewpoint, and choose a set of potential parameters originating a family of 2Y models characterized by (almost) the same shape of the attractive interaction, and in which the total strength of interactions (as measured by the second virial coefficient of the models) depends on the temperature but is held constant with respect to the choice of potential parameters. With this procedure, we aim to elucidate the connection between the features of the microscopic interaction (as e.g. the repulsion strength and range or shape of the attractive contribution), the properties of the aggregation process, and the **cluster** fluid thereby formed.

Our theoretical investigation is carried out in the framework provided by the Ornstein-Zernike integral equation theory of atomic fluids [41]. In particular, we have adopted two refined, thermodynamically self-consistent closure relations [42, 43], namely the Modified Hypernetted Chain (MHNC) scheme of Rosenfeld and Ashcroft [44] and a relation proposed by two of the authors (Bomont and Bretonnet, BB hereafter) [45, 46], interpolating via a consistency parameter between the Hypernetted Chain (HNC) [42, 43] and the Martynov-Sarkisov [47] closures. We again acknowledge the substantial contribution of Luciano Reatto and collaborators to the theoretical characterization of the fluid phase, as provided by the development of the Hierarchical Reference Theory [48] (see also [49, 50] for recent advances), and by refinements of the basic MHNC [51] and Optimized Random Phase approximations [52] theories.

The paper is organized as follows: in the next section we introduce the 2Y models, in Section 3 we report and discuss our results, last section contains the conclusions.

2. Model and theories

2.1. The two-Yukawa model

Two-Yukawa particles interact via the potential:

$$V(r) = \begin{cases} +\infty & r < \sigma \\ \frac{-K_1}{r/\sigma} \exp\left[-z_1\left(\frac{r}{\sigma} - 1\right)\right] + \frac{K_2}{r/\sigma} \exp\left[-z_2\left(\frac{r}{\sigma} - 1\right)\right] & r \geq \sigma. \end{cases} \quad (1)$$

The potential in Eq. (1) is characterized by a purely hard-core repulsion of diameter σ followed by an attractive well of strength and range K_1 and $1/z_1$, respectively, and by a repulsive tail at larger distances of strength and range K_2 and $1/z_2$, respectively. A short-range attraction followed by a long-range repulsion are obtained through the requirement $K_1 > K_2 > 0$ and $z_1 > z_2 > 0$. For $K_2 = 0$, a purely attractive Yukawa interaction is recovered, while assuming $K_2 = K_1 = 0$ leads to the familiar hard-sphere model. The hard-core diameter σ and the potential well depth $\varepsilon = (K_1 - K_2)$ provide, respectively, the natural distance and energy scales of the system. The reduced temperature is defined as $T^* = k_B T / \varepsilon$, where k_B is the Boltzmann constant.

A typical example of previous studies, drawn from our recent paper [36], is reported in Figure 1, where we show a family of 2Y models with z_1 , z_2 and K_1 held fixed and different K_2/K_1 ratios; as we have alluded to in the Introduction, though K_2/K_1 changes “systematically” between 0.01 and 0.1, the resulting poten-

tials do not vary “systematically”, making difficult the interpretation of structural and thermodynamics predictions in terms e.g. of the properties of the attractive well or in terms of the amplitude/decay of the repulsive tail. Here, first we have fixed the minimum of the potential as $V_{\min} \equiv V(r = \sigma) = -1$, and the distance r_0 whereupon the potential crosses zero i.e. $V(r = r_0) = 0$ as $r_0 = 1.1\sigma$. Both requirement can be satisfied by means of the two relations:

$$K_1 = \frac{1}{1 - \exp[(z_2 - z_1)(r_0 - \sigma)]} \quad (2)$$

$$K_2 - K_1 = -1. \quad (3)$$

As visible from Figure 2a (see also the magnification in the inset), this procedure produces almost similar, quite short-range shapes of the 2Y attractive contribution for a variety of different repulsive realizations. We shall discuss more in the Results section the implications of such small differences.

Secondly, we have required that the total interaction strength is fixed, independently on the choice of a particular set of parameters. A natural way to define an “integrated measure” of interactions is provided by the second virial coefficient,

$$B_2(T^*) = B_2^{\text{HS}} + B_2^{\text{soft}}(T^*) = -\frac{2}{3}\pi\sigma^3 - 2\pi \int_{\sigma}^{\infty} \{\exp[-\beta V(r)] - 1\} r^2 dr, \quad (4)$$

where $\beta = 1/T^*$ and B_2 has been expressed as a sum of the hard-core and soft contributions. The expression in Eq. (4) depends on the temperature; nevertheless, as visible in Figure 2b, once a particular value of z_1 has been fixed, the same behaviour of $B_2^{\text{soft}}/B_2^{\text{HS}}$ as a function of T^* can be enforced on a given temperature interval, with an appropriate choice of z_2 (see also the inset, showing an almost linear scaling of B_2 vs T on a log-log scale). **In particular, we have chosen three different z_1 values (i.e. $z_1 = 19$, model M1 hereafter; $z_1 = 13$, model M2; $z_1 = 10$, model M3) and freely fixed $z_2 = 0.5$ for $z_1 = 10$, as in Ref. [36]; then, we have identified the remaining two z_2 values (to within a $\Delta z_2 = 0.001$ resolution) as those minimizing the variance between the various B_2 in the temperature range $[0.4 - 0.8]$.** Numerical values of all parameters of the three 2Y models, plotted in Figure 2b, are given in Table 1. The models span a reasonably wide interval of the height-to-depth ratio of the 2Y potential, ranging from $\sim 13\%$ to $\sim 36\%$ (see the last column in Table 1). The small discrepancies among various B_2 visible in Figure 2b do not influence the system properties around the temperature threshold for the cluster formation. In fact, such discrepancies emerge (by construction) for $T^* \lesssim 0.4$ and $T^* \gtrsim 0.8$, where preliminary calculations have shown that clusters are either already well developed (at low T^*) or still completely absent (at high T^*). The equivalence of B_2 implies that the increase of the repulsive barrier is tempered at each temperature by a quicker decay of $V(r)$ at long distances.

2.2. Liquid state theories

The properties of the 2Y models are calculated in the framework provided by integral equation theories of the liquid state. The starting point is the Ornstein-Zernike equation [41], providing an exact relationship between the total correlation function of the fluid $h(r) = g(r) - 1$ [where $g(r)$ is the pair distribution function]

and the direct correlation function $c(r)$ in the form:

$$h(r) = c(r) + \rho \int c(|r - r'|) h(r') dr', \quad (5)$$

where ρ is the number density. Eq. (5) must be supplemented by a closure relation, derived from cluster diagrammatic analysis, that reads:

$$g(r) = \exp[-\beta V(r) + \gamma(r) + B(r)], \quad (6)$$

where $\gamma(r) = h(r) - c(r)$ is the indirect correlation function; the various “ansatz” proposed to approximate the unknown bridge function $B(r)$ are at the heart of different integral equation approaches [42, 43]. In this work we have applied the MHNC scheme, in which $B(r)$ is approximated by the bridge function of the hard-sphere (HS) system, following a prescription based on the universality in the short-range structure observed in a wide class of model fluids [44]. We have used in particular the Verlet-Weis (VW) parametrization of simulation data [53], i.e.

$$B(r) \equiv B_{\text{HS}}^{\text{VW}}(r, \sigma_{\text{HS}}) \quad (\text{MHNC}), \quad (7)$$

with the hard-core diameter σ_{HS} fixed so to enforce the thermodynamic self-consistency of the theory, as given by the equality between the isothermal compressibilities calculated from the virial and compressibility routes from structure to thermodynamics [41],

$$\beta \left. \frac{\partial P^{\text{vir}}}{\partial \rho} \right|_{T, \rho} = 1 - \rho \int c(r) dr, \quad (8)$$

where

$$P^{\text{vir}} = \rho k_{\text{B}} T - \frac{2}{3} \pi \rho^2 \int r^3 g(r) \frac{dV(r)}{dr} dr. \quad (9)$$

An application of a simplified, thermodynamically non-consistent MHNC scheme to 2Y fluids — with $B(r)$ in Eq. (7) given by the Percus-Yevick expression for the hard-sphere fluid bridge function at the same density [42, 43] — is also reported in Ref. [20].

As for the second closure, the bridge function reads [45, 46]:

$$B(r) = [1 + 2\gamma(r) + f\gamma^2(r)]^{1/2} - 1 - \gamma(r) \quad (\text{BB}); \quad (10)$$

as mentioned in the Introduction, the proposed expression for $B(r)$ interpolates between the basic HNC approximation, $B(r) = 0$, recovered when the mixing parameter f is set equal to one, and the Martynov-Sarkisov closure [47], obtained when $f = 0$. It is important to note that neither the HNC nor the Martynov-Sarkisov schemes are thermodynamically consistent, whereas in the BB procedure the mixing parameter f is again determined so to enforce the thermodynamic consistency condition of Eq. (8).

The Gillan [54] and Labik *et al.* [55] numerical iterative algorithms have been used to solve the Ornstein-Zernike equation coupled with the MHNC and BB closures, respectively. We have calculated all correlation functions on an extended and finely resolved grid of 2^{14} points with $\Delta r = 0.005\sigma$, covering a spatial range of 81.92σ .

We have ensured in this way an accurate treatment of the long-range behaviour of various correlation functions, as well as a precise characterization of the k -space properties via Fourier inversion.

3. Results and discussion

As a first step, we have verified the accuracy of MHNC structural predictions for the 2Y fluid. To date, in fact, only a simplified, thermodynamically non-consistent version of MHNC was applied in context of 2Y fluids [20], in an attempt to predict the liquid-vapour phase coexistence. In Figure 3 we have compared the MHNC structure factors $S(k)$ with the corresponding Monte Carlo data reported in our previous work [36]. As visible, MHNC gives practically quantitative structural predictions, performing only slightly better than BB in the **cluster fluid** (see also the inset). The accuracy of MHNC predictions — together with the already known evidences for BB [36] and HMSA [40] — further confirms that refined, self-consistent integral equation theories provide a reliable tool to investigate the properties of models with competing interactions and the properties of the **cluster fluids they are able to form** [40].

In order to approximately locate a scale of temperatures relevant for the phase behaviour, we have applied the Noro-Frenkel rule of corresponding states [56] to predict the critical temperature of the attractive parts only of the three 2Y models [as obtained for instance by setting $V(r > r_0) = 0$ in the full potential of Eq. (1)]. **The empirical rule determined by Noro and Frenkel in Ref. [56] — well verified by a wide class of central potentials — states a linear relationship between the range of a given interaction potential and the corresponding critical temperature, once (i) the critical temperature is expressed in terms of the depth of the potential well (as in our previous definition of T^*) and (ii) the range of the potential is expressed in terms of an equivalent square-well interaction having the same reduced second virial coefficient $B_2(T^*)/B_2^{\text{HS}}$ [see Eq. (4)] at the same reduced temperature T^* .** The Noro-Frenkel rule predicts critical temperatures for the models at issue around $T_{\text{cr}}^* = 0.30$; specifically, due to the small differences in the overall shape of the attractive part discussed in the previous section, we have obtained $T_{\text{cr}}^* = 0.291$, 0.297, and 0.301 for model M1, M2 and M3, respectively, coherently with the fact that the wider the attractive well (see inset of Figure 2), the higher the liquid-vapour critical temperature. The same rule also predicts for all 2Y models of Table 1 that the attractive contribution is short-range enough to result in a liquid-vapour phase separation metastable with respect to the vapour-solid coexistence. We have also tried to calculate the whole liquid-vapour binodal, unfortunately concluding that both MHNC and BB schemes fail to provide a numerical solution in a relatively large region comprising the binodal (a similar conclusion has been drawn also in Ref. [21] for the simpler HNC and MHNC schemes therein adopted); we can only say that as T^* is lowered towards T_{cr}^* , the MHNC compressibility becomes progressively structured and exhibits a maximum, as a function of the density, placed around $\rho\sigma^3 \approx 0.42$, reasonably providing an approximate indication of the critical density.

As the repulsive part of the 2Y model is switched on, resulting in the whole expression of Eq. (1), the liquid-vapour metastable separation concerning the attractive part is definitely suppressed in favour of the aggregate formation, according to the competition mechanism between microsegregation and condensation already described in the Introduction. In particular, the analytical Mean Spherical Approximation predicts — as the more refined Self-Consistent Ornstein-Zernike Approximation

mation equally does [14] — that the liquid-vapour binodal disappears when

$$\frac{K_2}{K_1} > \left(\frac{z_1}{z_2} \right)^2 \left[\frac{z_2 - 2 + (z_2 + 2) e^{-z_2}}{z_1 - 2 + (z_1 + 2) e^{-z_1}} \right]^2, \quad (11)$$

a condition largely satisfied for all parametrizations of Table 1.

We have generated theoretical predictions concerning the three models of Table 1 at three different packing fractions spanning the fluid regime, namely $\eta \equiv \pi\rho\sigma^3/6 = 0.10, 0.20$ and 0.25 . For opportunity reasons, we have worked on an equally spaced grid in β , i.e. the inverse of the reduced temperature, with a resolution as fine as $\Delta\beta = 0.01$. The appearance of the cluster peak has been identified with the development of a local low- k maximum in $S(k)$. The corresponding $\beta_{\text{cluster}} = 1/T_{\text{cluster}}^*$ has been taken as the one halfway the two sequential β values whereupon such maximum first develops, to within the resolution adopted; we have then estimated the theoretical uncertainty as $\Delta\beta/2$.

In figure 4 we have reported the MHNC and BB $S(k)$ for all 2Y models, at fixed $\eta = 0.20$, starting from low β values, passing across the cluster formation threshold up to β regimes where the **cluster fluid** definitely sets in. As visible, MHNC and BB theories agree in the normal fluid regime, whereas BB predicts slightly enhanced cluster-cluster correlations as the temperature is lowered, resulting in slightly higher T_{cluster}^* in comparison with the MHNC ones. The cluster formation involves a shift of the main peak toward higher k values, signalling the onset of a shorter characteristic length scale of monomer-monomer correlations, in comparison with the **normal** fluid phase. In particular, as already observed in our previous work [36], this indicates that clusters become more compact as the temperature is reduced; at the same time the cluster peak **develops significantly** with decreasing the temperature and slightly shifts to lower wavevectors. The cluster peak in Figure 4 moves towards higher wavevectors as the barrier height increases, consistently with earlier evidence reported in Ref. [38]. The way in which our 2Y models are built implies that higher barriers correspond to quicker decays of the repulsive interactions (see Figure 2a). In this sense, we interpret the above mentioned shift as signalling that a larger characteristic intercluster correlation distance sets in the fluid, as the overall repulsive background becomes progressively broader and longer-ranged, i.e. in passing from Model 3 to Model 1. **As visible from Figure 4, while the lower temperatures at which the structure factor is studied are close to or even lower than the critical temperatures of the purely attractive fluid estimated by the Noro-Frenkel rule, the $k \rightarrow 0$ limit of the structure factor, directly related to the isothermal compressibility, always remains much lower than unity. This evidence (together with the fact that the second virial coefficient is always positive, see Figure 2b), further corroborates our previous statement about the absence of a liquid-vapour phase separation. On the other hand, since our models have a long-range repulsive contribution (non negligible up to $r \sim 4\sigma$), the system is expected to form [29], for low enough temperatures, a Wigner glass of clusters, i.e. a disordered state of polydisperse clusters that do not percolate to give a gel. The investigation of this regime is substantially out of the scope of the theoretical framework employed in this work; moreover, as shown in Ref. [36], the BB algorithm ceases to numerically converge for temperatures approximately around $T^* = 0.30$ (i.e. close to the lowest temperatures reported in Figure 4), and test calculations (not reported here) demonstrate that the same limiting temperature range holds for the MHNC approximation.**

In Figure 5, the MHNC and BB predictions for T_{cluster}^* are reported as a function of $V_{\text{max}}/\varepsilon$, i.e. the ratio between the height of the repulsive barrier and the

potential well depth (see Table 1). The dependence of T_{cluster}^* on such ratio appears almost linear, with a close agreement emerging between the two theories. Moreover, the higher is the potential barrier, the higher is the threshold temperature (at fixed packing fraction) for the cluster formation. This proportionality suggests that the onset of the microsegregation process sensitively depends on the competition between thermal energy and potential barrier: as the temperature decreases they become comparable to each other, the cluster seeds (constituted by a central particle and its first neighbours sensing the potential attractive well) are progressively stabilized against the thermal motion, and the aggregate formation can take place. The increase of T_{cluster}^* with the barrier height is at variance with the opposite trend emerged in Ref. [36]; we note in this instance that the 2Y parametrization adopted in [36] did not have a unique attractive potential well, as we have deliberately constructed in the present work. Indeed, in that case, the highest potential barrier was associated to the narrowest attractive well (see Figure 1, reproducing the models adopted in Ref. [36]); it then possibly turned out necessary to emphasize attractions, that is to reduce the temperature, in order to promote the cluster formation.

In Figure 6 the temperature T_{cluster}^* for all models is shown as a function of the packing fraction η . The observed decrease of T_{cluster}^* vs η has already been signalled in Refs. [36, 37]. A plausible explanation is that at higher packings the formation of clusters is hampered by the strong repulsion, with the system dominated by single-particle dynamics [37], so that attractive potential effects must be emphasized, as it happens when T^* is lowered.

All numerical values of β_{cluster} are conclusively reported in Table 2. As can be deduced also from previous Figures 5 and 6, MHNC and BB predictions are discrepant from each other by no more than 3%. As for the achievement of very accurate thermodynamic consistency conditions, the BB solution algorithm appears more successful than the MHNC one. In fact the thermodynamic consistency in Eq. (8) must be enforced with different degrees of accuracy, in order to ensure the convergence of the numerical schemes. It turns out that, while for the BB closure a very accurate 0.05% consistency can be achieved for all system and densities investigated, a less stringent 1% requirement is generally needed for the MHNC, rising to 2-3% for the lowest temperatures investigated, specifically those concerning Model 1.

4. Conclusions

We have applied two accurate integral equation theories of the liquid state to characterize the cluster formation threshold — as a function of the temperature and for three densities spanning the fluid phase — in two-Yukawa fluids exhibiting microscopic competing interactions. Specifically, we have used the MHNC theory and another closure to the Ornstein-Zernike equation proposed by two of the authors (named BB in the text), interpolating in a thermodynamically self-consistent way between the simpler HNC and Martynov-Sarkisov approximations. We have studied a family of 2Y models characterized by almost the same attractive well, and in which the overall interaction strength (as exemplified by the second virial coefficient) scales in the same way with the temperature over a range comprising the cluster temperature for all models, independently on the choice of potential parameters. In this way, we have related the onset of microsegregation with few fixed general features of the microscopic interactions as e.g. height and decay of the potential barrier. By contrast, most of previous studies were based on a systematic variation of potential parameters, not necessarily reflecting into a corresponding

systematic variation of the properties of the 2Y interaction. We have profited from using the theoretical approach to study the various 2Y models over a considerable spatial extension and a finely resolved temperature grid; we have in this way accurately predicted the temperatures whereupon the 2Y fluid transforms into a “cluster fluid” with almost negligible theoretical uncertainties.

We have initially verified that, in substantial agreement with BB predictions, the MHNC theory accurately reproduces the Monte Carlo structural correlation calculated in a previous work. We have then approximately calculated the liquid-vapour critical point of the common attractive part of all models. Due to the short-range nature of attractive interactions, the liquid-vapour coexistence is only metastable with respect to the fluid-solid phase separation, and completely disappears in favour of the microsegregation once the full 2Y interaction is taken into account. We have found that the cluster temperature scales almost linearly with the height of the repulsive interactions, over a variety of different model realizations and fluid densities. Specifically, the temperature threshold moves toward higher temperatures as the height of the barrier increases. Once the cluster fluid is stabilized, the position of the cluster peak in the structure factor corresponds to correlation distances in r -space that increase as the interaction range increases, with a correspondingly lower repulsive barrier. Works trying to better elucidate the interplay between the features of the competing interactions and **properties of the cluster fluid** are currently in progress.

References

- [1] A. Stradner, H. Sedgwick, F. Cardinaux, W. C. Poon, S. U. Egelhaaf, and P. Schurtenberger, *Nature (London)* **432**, 492 (2004).
- [2] Y. Liu, E. Fratini, P. Baglioni, W. R. Chen, and S.-H. Chen, *Phys. Rev. Lett.* **95**, 118102 (2005).
- [3] F. Cardinaux, A. Stradner, P. Schurtenberger, F. Sciortino, and E. Zaccarelli, *Europhys. Lett.* **77**, 48004 (2007).
- [4] A. Shukla, E. Mylonas, E. Di Cola, S. Finet, P. Timmins, T. Narayanan, and D. I. Svergun, *Proc. Natl. Acad. Sci. (USA)* **105**, 5075 (2008).
- [5] Y. Liu, L. Porcar, J. Chen, W.-R. Chen, P. Falus, A. Faraone, E. Fratini, K. Hong, and P. Baglioni, *J. Phys. Chem. B* **115**, 7238 (2011).
- [6] J. Groenewold and W. K. Kegel, *J. Phys.: Condens. Matter* **16**, S4877 (2004).
- [7] A. I. Campbell, V. J. Anderson, J. S. van Duijneveldt, and P. Bartlett, *Phys. Rev. Lett.* **94**, 208301 (2005).
- [8] F. Lo Verso, C. N. Likos, and L. Reatto, *Prog. Colloid Polym. Sci.* **133**, **78** (2006).
- [9] J.-L. Barrat and J.-P. Hansen, *Basic Concepts for Simple and Complex Liquids* (Cambridge University Press, Cambridge, 2003).
- [10] A. Tardieu, S. Finet, and F. Bonneté, *J. Cryst. Growth* **232**, 1 (2001).
- [11] A. A. Louis, E. Allahyarov, H. Löwen, and R. Roth, *Phys. Rev. E* **65**, 061407 (2002).
- [12] D. Bonn, J. Otwinowski, S. Sacanna, H. Guo, G. Wegdam, and P. Schall, *Phys. Rev. Lett.* **103**, 156101 (2009).
- [13] M. Seul and D. Andelman, *Science* **267**, 476 (1995).
- [14] D. Pini, G. Jialin, A. Parola, and L. Reatto, *Chem. Phys. Lett.* **327**, 209 (2000).
- [15] D. Pini, A. Parola, and L. Reatto, *J. Phys.: Condens. Matter* **18**, S2305 (2006).
- [16] A. J. Archer, C. Ionescu, D. Pini, and L. Reatto, *J. Phys.: Condens. Matter* **20**, 415106 (2008).
- [17] A. Imperio and L. Reatto, *J. Phys.: Condens. Matter* **16**, S3769 (2004).
- [18] A. Imperio, L. Reatto, and S. Zapperi, *Phys. Rev. E* **78**, 021402 (2008).
- [19] A. J. Archer, D. Pini, R. Evans, and L. Reatto, *J. Chem. Phys.* **126**, 014104 (2007).
- [20] A. J. Archer and N. B. Wilding, *Phys. Rev. E* **76**, 031501 (2007).
- [21] A. J. Archer, *Phys. Rev. E* **78**, 031402 (2008).
- [22] M. Tarzia and A. Coniglio, *Phys. Rev. Lett.* **96**, 075702 (2006).
- [23] M. Tarzia and A. Coniglio, *Phys. Rev. E* **75**, 011410 (2007).
- [24] A. Ciach, *Phys. Rev. E* **78**, 061505 (2008).
- [25] A. Ciach and W. T. Gózdź, *Cond. Matt. Phys.* **13**, 23603 (2010).
- [26] A. Ciach, *Molec. Phys.* **109**, 1101 (2011).
- [27] P. Baglioni, E. Fratini, B. Lonetti, and S.-H. Chen, *J. Phys.: Condens. Matter* **16**, S5003 (2004).
- [28] J. Wu, Y. Liu, W. R. Chen, J. Cao, and S.-H. Chen, *Phys. Rev. E* **70**, 050401 (2004).
- [29] F. Sciortino, S. Mossa, E. Zaccarelli, and P. Tartaglia, *Phys. Rev. Lett.* **93**, 055701 (2004).
- [30] B. Lonetti, E. Fratini, S.-H. Chen, and P. Baglioni, *Phys. Chem. Chem. Phys.* **6**, 1388 (2004).
- [31] F. Sciortino, P. Tartaglia, and E. Zaccarelli, *J. Phys. Chem. B* **109**, 21942 (2005).
- [32] P. J. Lu, J. C. Conrad, H. M. Wyss, A. B. Schofield, and D. A. Weitz, *Phys. Rev. Lett.* **96**, 028306 (2006).

- 1 [33] P. J. Lu, E. Zaccarelli, F. Ciulla, A. B. Schofield, F. Sciortino, and D. A. Weitz, *Nature (London)* **453**,
2 499 (2008).
- 3 [34] J. C. F. Toledano, F. Sciortino, and E. Zaccarelli, *Soft Matter* **5**, 2390 (2009).
- 4 [35] R. P. Sear and W. M. Gelbart, *J. Chem. Phys.* **110**, 4582 (1999).
- 5 [36] J.-M. Bomont, J.-L. Bretonnet, and D. Costa, *J. Chem. Phys.* **132**, 184508 (2010).
- 6 [37] Y. Liu, W.-R. Chen, and S.-H. Chen, *J. Chem. Phys.* **122**, 044507 (2005).
- 7 [38] M. Broccio, D. Costa, Y. Liu, and S.-H. Chen, *J. Chem. Phys.* **124**, 084501 (2006).
- 8 [39] L. L. Lee, M. C. Hara, S. J. Simon, F. S. Ramos, A. J. Winkle, and J.-M. Bomont, *J. Chem. Phys.*
9 **132**, 074505 (2010).
- 10 [40] J.M. Kim, R. Castañeda-Priego, Y. Liu, and N. J. Wagner, *J. Chem. Phys.* **134**, 064904 (2011).
- 11 [41] J.-P. Hansen and I. R. McDonald, *Theory of Simple Liquids*, 2nd ed. (Academic Press, London, 1986).
- 12 [42] C. Caccamo, *Phys. Rep.* **274**, 1 (1996).
- 13 [43] J.-M. Bomont, *Adv. Chem. Phys.* **39**, 1 (2008).
- 14 [44] Y. Rosenfeld and N. W. Ashcroft, *Phys. Rev. A* **20**, 1208 (1979).
- 15 [45] J.-M. Bomont, *J. Chem. Phys.* **119**, 11484 (2003).
- 16 [46] J.-M. Bomont and J.-L. Bretonnet, *J. Chem. Phys.* **121**, 1548 (2004).
- 17 [47] G. A. Martynov and G. N. Sarkisov, *Mol. Phys.* **49**, 1495 (1983).
- 18 [48] A. Parola and L. Reatto, *Adv. Phys.* **44**, 211 (1995).
- 19 [49] A. Parola, D. Pini, and L. Reatto, *Phys. Rev. Lett.* **100**, 165704 (2008).
- 20 [50] D. Pini, F. Lo Verso, M. Tau, A. Parola, and L. Reatto, *Phys. Rev. Lett.* **100**, 055703 (2008).
- 21 [51] S. M. Foiles, N. W. Ashcroft, and L. Reatto, *J. Chem. Phys.* **80**, 4441 (1984).
- 22 [52] D. Pini, A. Parola, and L. Reatto, *Molec. Phys.* **100**, 1507 (2002).
- 23 [53] L. Verlet and J. J. Weis, *Phys. Rev.* **45**, 939 (1972).
- 24 [54] M. J. Gillan, *Mol. Phys.* **38**, 1781 (1979).
- 25 [55] S. Labik, A. Malijeovski, and P. Vonka, *Mol. Phys.* **56**, 709 (1985).
- 26 [56] M. G. Noro and D. Frenkel, *J. Chem. Phys.* **113**, 2941 (2000).
- 27
- 28
- 29
- 30
- 31
- 32
- 33
- 34
- 35
- 36
- 37
- 38
- 39
- 40
- 41
- 42
- 43
- 44
- 45
- 46
- 47
- 48
- 49
- 50
- 51
- 52
- 53
- 54
- 55
- 56
- 57
- 58
- 59
- 60

TABLES

Table 1. Parameters of the three 2Y potentials shown in Figure 2a. r_{\max} and v_{\max} are, respectively, the position and height of the (finite) maximum of the potential.

| Model | z_1 | z_2 | K_1 | K_2 | r_{\max}/σ | V_{\max}/ε |
|-------|-------|-------|--------|--------|-------------------|------------------------|
| M1 | 19 | 0.257 | 1.1813 | 0.1813 | 1.256 | 0.128 |
| M2 | 13 | 0.390 | 1.3954 | 0.3954 | 1.297 | 0.249 |
| M3 | 10 | 0.500 | 1.6306 | 0.6306 | 1.326 | 0.357 |

Table 2. MHNC and BB β_{cluster} . The error bars amount to 0.005, i.e. half the mesh size in β . The attainable thermodynamic consistency for each model and each packing fraction is indicated by the superscripts: ‡ = 0.05%; † = 1%; § = 2% ¶ = 3%.

| Model | MHNC | | | BB | | |
|-------|--------------------|--------------------|--------------------|--------------------|--------------------|--------------------|
| | $\eta = 0.10$ | $\eta = 0.20$ | $\eta = 0.25$ | $\eta = 0.10$ | $\eta = 0.20$ | $\eta = 0.25$ |
| M1 | 2.395 [§] | 2.545 [¶] | 2.615 [¶] | 2.355 [‡] | 2.505 [‡] | 2.595 [‡] |
| M2 | 1.875 [†] | 1.985 [†] | 2.085 [†] | 1.865 [‡] | 1.965 [‡] | 2.035 [‡] |
| M3 | 1.515 [†] | 1.645 [†] | 1.735 [†] | 1.485 [‡] | 1.595 [‡] | 1.695 [‡] |

FIGURE CAPTIONS

Figure 1. The 2Y models studied in Ref. [36] with $z_1 = 10$, $z_2 = 0.5$ and $[1/K_1; K_2/K_1] = [0.9; 0.1]$ (full line); $[0.95; 0.05]$ (dashed line); $[0.99; 0.01]$ (dotted line). The inset contains a magnification of the region around the repulsive barrier.

Figure 2. (a) The family of 2Y potentials deduced according to the requirements described in the text (inset: magnification of the attractive part) and (b) corresponding second virial coefficients as a function of the reduced temperature (inset: same plot on a log-log scale). See Table 1 for numerical values of K_1 , K_2 , z_1 and z_2 .

Figure 3. Comparison between MHNC predictions and MC data [36] for a 2Y model with $1/K_1 = 0.9$, $K_2/K_1 = 0.10$, $z_1 = 10$ and $z_2 = 0.5$ at a packing fraction $\eta \equiv \pi\rho\sigma^3/6 = 0.15$ and different temperatures across the cluster formation threshold. BB predictions [36] are also reported for completeness. Inset: magnification of the cluster peak region.

Figure 4. Structure factors of the three models investigated in this work at various temperature and fixed packing fraction $\eta = 0.20$. Model M1 (top panel): $\beta = 0.10, 2.54, 2.55$ and 3.0 for MHNC and $\beta = 0.10, 2.50, 2.51$ and 3.0 for BB. Model M2 (central panel): $\beta = 1.2, 1.98, 1.99$, and 2.5 for MHNC and $\beta = 1.2, 1.96, 1.97$, and 2.5 for BB. Model M3 (bottom panel): $\beta = 0.10, 1.64, 1.65$ and 2.0 for MHNC and $\beta = 0.10, 1.59, 1.60, 2.0$ for BB. β increases (i.e. T^* decreases) in the direction of the arrows. Insets: magnification of the cluster peak region.

Figure 5. T_{cluster}^* as a function of the height-to-depth ratio of 2Y potentials (see Table 1) and packing fractions $\eta = 0.10, 0.20$ and 0.25 . Full symbols and full lines: MHNC predictions and corresponding linear bestfits. Open symbols and dashed lines: BB predictions and corresponding linear bestfits. Error bars on T_{cluster}^* are of the order of the size of the symbols.

Figure 6. T_{cluster}^* as a function of the packing fraction η for all models investigated in this work. The estimated critical point of the attractive part only is also displayed (cross). BB and MHNC predictions are indistinguishable on the scale of the figure.

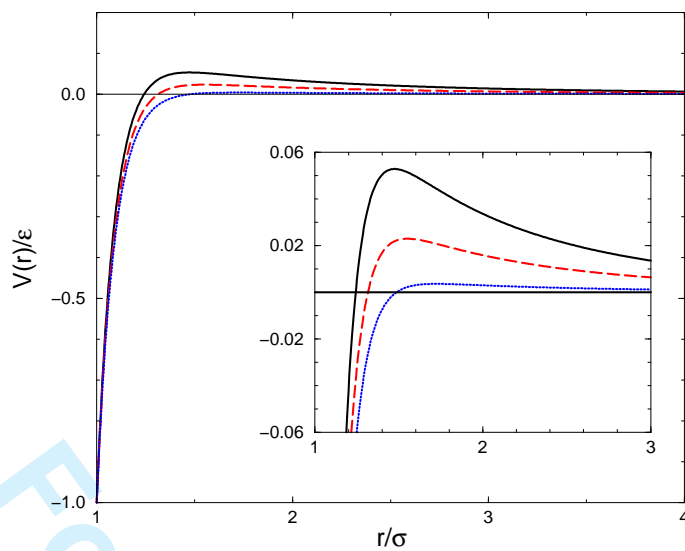
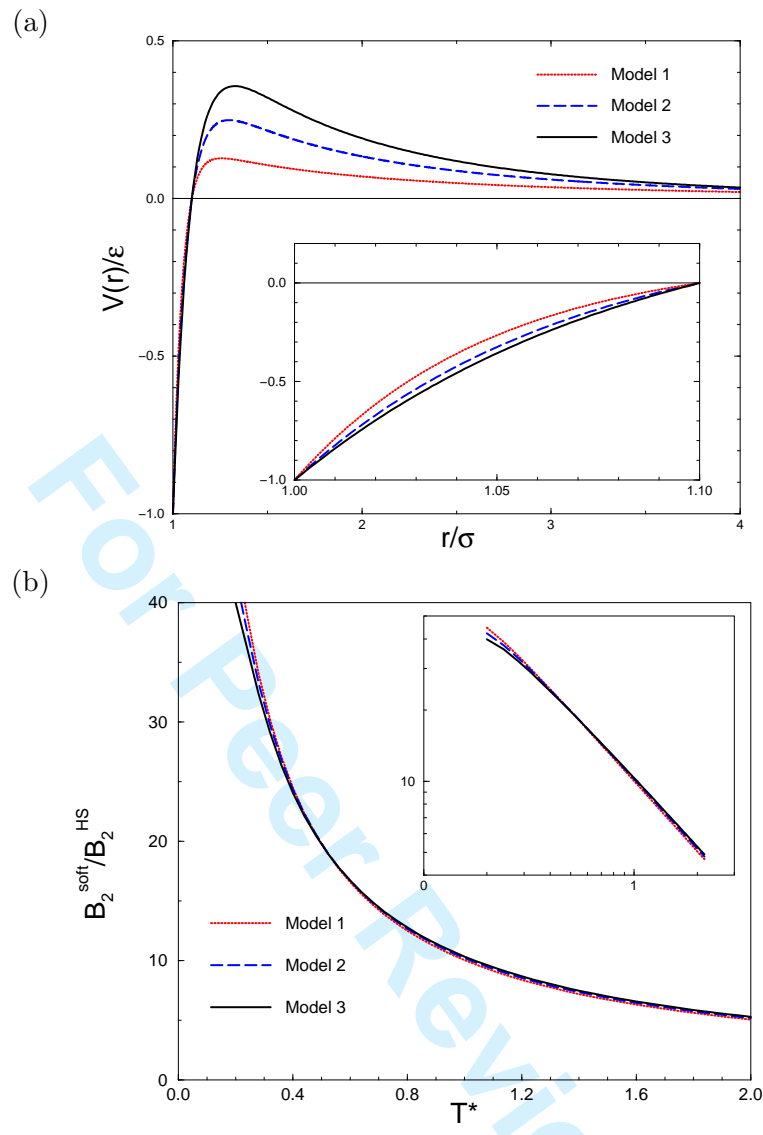


Figure 1.

For Peer Review Only

1
2
3
4
5
6
7
8
9
10
11
12
13
14
15
16
17
18
19
20
21
22
23
24
25
26
27
28
29
30
31
32
33
34
35
36
37
38
39
40
41
42
43
44
45
46
47
48
49
50
51
52
53
54
55
56
57
58
59
60



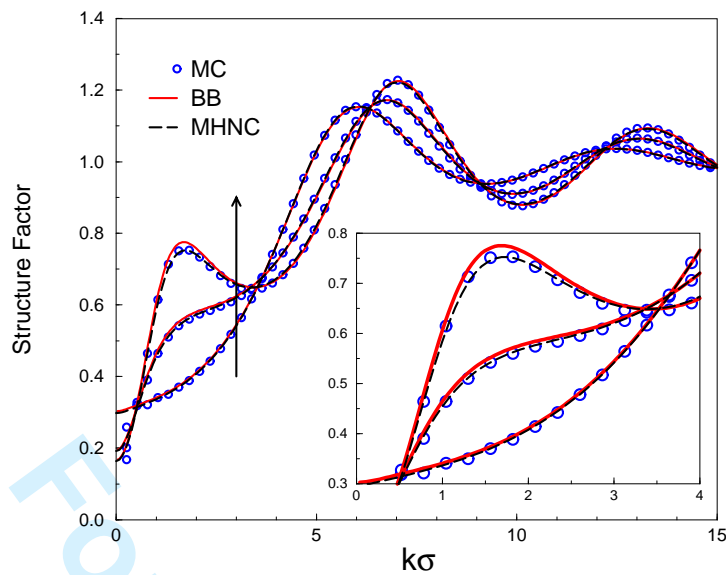


Figure 3.

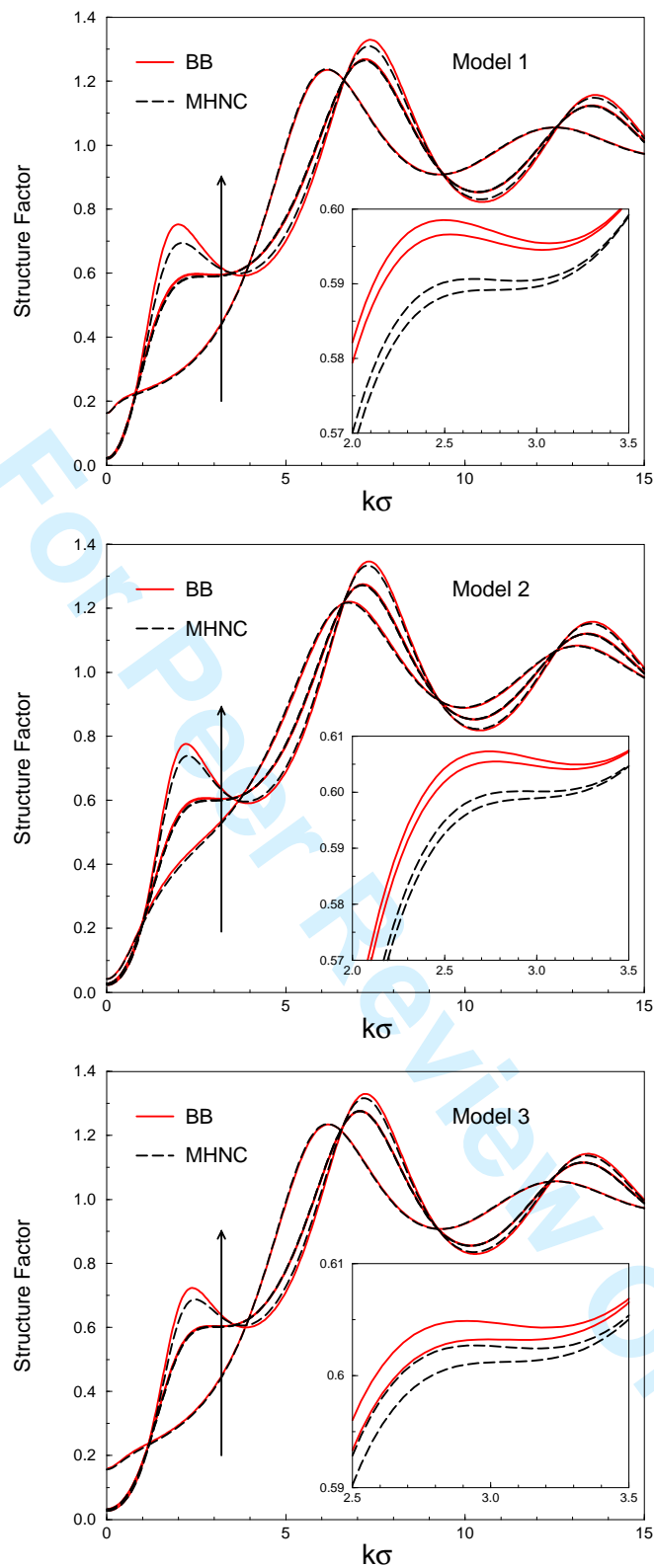


Figure 4.

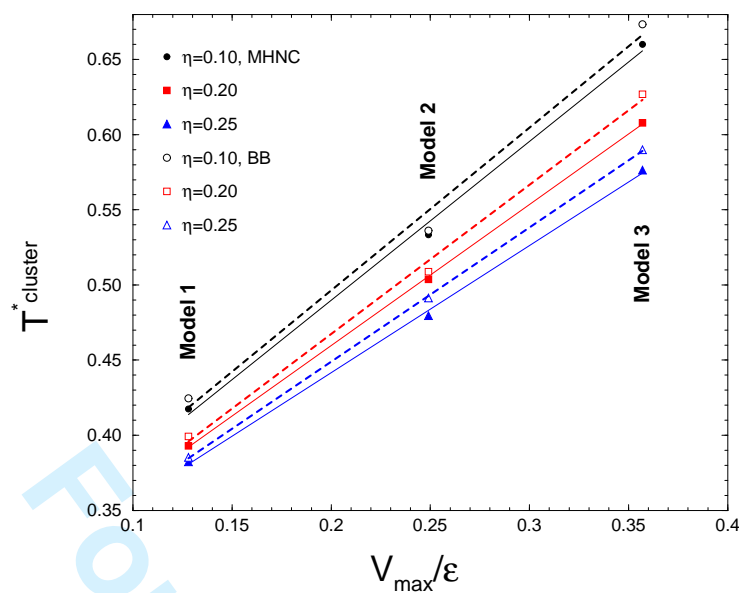


Figure 5.

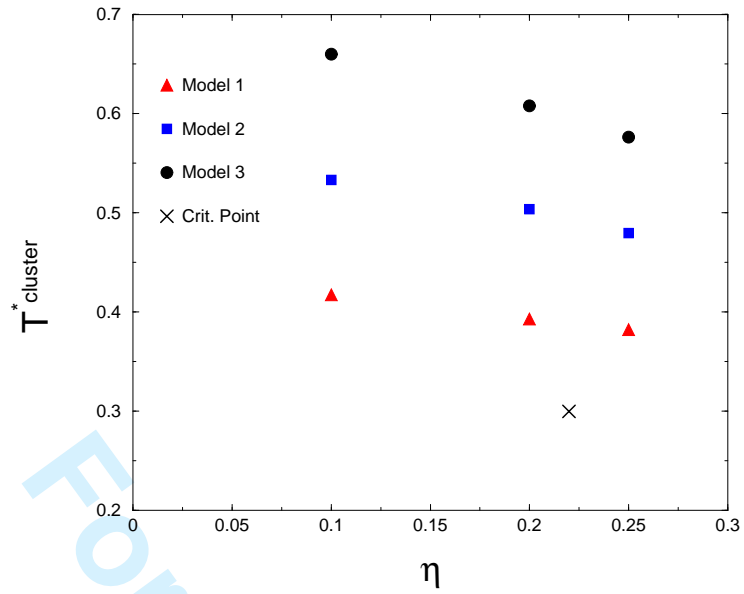


Figure 6.

For Peer Review Only